Continental Shelf Research 165 (2018) 120–136

Contents lists available at ScienceDirect

Continental Shelf Research

journal homepage: www.elsevier.com/locate/csr

Research papers

Dynamic equilibrium of sandbar position and height along a low wave energy micro-tidal coast

Jun Cheng*, Ping Wang

School of Geosciences, University of South Florida, Tampa, FL 33620, USA

ARTICLE INFO

Keywords:
Sandbar migration
Beach erosion
Seasonal beach cycle
Storm
Nearshore sediment transport
West-central Florida

ABSTRACT

Nearshore sandbars play an essential role in dissipating incident wave energy and protecting the beach landward. Thus, understanding the dynamic equilibrium of nearshore bars is valuable to beach management and shore protection. This study examines the sandbar equilibrium in terms of bar height and cross-shore bar location, in order to assess how the dynamic equilibrium is maintained and influenced by storms along a low wave energy micro-tidal coast. The bar height and bar position were extracted from 51 beach profiles surveyed every two months, spaced at 300 m along a 15-km stretch of beach from October 2010 to August 2014. For the studied coast, alongshore variation in equilibrium bar position measured from the shoreline ranges between 40 and 80 m and equilibrium bar height between 0.20 and 0.70 m. Greater equilibrium sandbar height tends to occur around a headland, where waves are higher. Alongshore variations of bar behavior were observed during storms, with both onshore and offshore bar migration observed during one storm. Water depth over the pre-storm sandbar crest is a major factor controlling the storm-induced onshore or offshore bar migration. On average, the depth over the onshore migrating sandbar is found to be 0.20 m deeper than that over the offshore migrating bar during both summer and winter storms. There is no significant correlation between incident wave angle and sandbar height changes, while significant correlation exists between wave angle and sandbar movement under certain wave conditions, with more oblique waves being associated with further offshore movement of the sandbar. Energetic storm conditions tend to make the bar higher than the equilibrium height, while post-storm adjustment would restore the equilibrium height within 4–6 months. Although the exact values may vary at different locations, the concept of dynamic equilibrium of bar height and distance to shoreline could apply at many locations.

1. Introduction

The sandbar and trough features are important parts of a nearshore equilibrium profile (Wang and Davis, 1998), and they have important implications on the performance of beach and nearshore nourishments (Kroon et al., 1994; Van Duin et al., 2004; Roberts and Wang, 2012; Brutsché et al., 2014). By inducing wave breaking, the nearshore bars reduce the incident wave energy arriving at the shoreline and therefore provide protection against beach erosion. Due to their control on wave breaking, sandbars influence the spatial distribution of turbulent kinetic energy generated by breaking waves as they propagate onshore (Longo et al., 2002; Cheng and Wang, 2015a). Nearshore water quality can also be influenced by the existence of sandbars (Feng et al., 2013). Thus, understanding and quantifying the sandbar behavior play an important role in coastal management and shore protection. Sandbar morphodynamics remains a challenging research topic due to complicated interaction between breaking waves and sediment transport in the energetic surf zone (Voulgaris and Collins, 2000; Ruessink and Kuriyama, 2008).

Time-series of beach profile surveys along a significant stretch of coast, e.g., on the order of tens of kilometers, are essential to quantifying the temporal and spatial behavior of beach-sandbar system (Browder and Dean, 2000; Roberts and Wang, 2012). However, long-term field measurements of sandbar configurations (e.g. bar height and bar location) and their response to incident wave conditions are limited to a few locations (Ruggiero et al., 2009). Well known examples include Duck, North Carolina, USA (Holman and Sallenger, 1993; Larson et al., 2000; Plant et al., 2001), Egmond, Netherlands (Ruessink et al., 2000; Pape et al., 2010), Hasaki, Kashima Coast, Japan (Kuriyama et al., 2008), and Gold Coast, Australia (Castelle et al., 2007). Most of these well studied coasts have multiple nearshore sandbars in the surf zone and cyclic cross-shore bar migration occurs. Such a cycle is typically characterized by a net offshore bar migration (NOM) comprising sandbar generation near the shoreline by a storm, followed by a period of offshore bar migration, and eventual bar decay at the seaward edge

* Corresponding author.
E-mail address: jun@mail.usf.edu (J. Cheng).

https://doi.org/10.1016/j.csr.2018.05.004
Received 6 July 2016; Received in revised form 10 May 2018; Accepted 11 May 2018
Available online 13 May 2018
0278-4343/

of the breaker zone (Kuriyama et al., 2008; Ruessink et al., 2000). Field studies on nearshore sandbar behavior along low-energy coasts are scarce and the applicability of findings from multibarred and high-energy coasts along low-energy micro-tidal coasts is not clear. A few existing examples include research conducted at the fetch limited Mediterranean Sea (Guillén and Palanques, 1993; Certain and Barusseau, 2005; Ojeda et al., 2011). General cyclic morphological behavior with interruption from severe storm events was documented along those coasts. Compared to previous studies at high-energy coasts, the morphological response of low-energy micro-tidal coasts is more sensitive to changing wave conditions (Aleman et al., 2015).

Several numerical modeling studies have revealed some insights on the mechanisms of sandbar height change and its cross-shore movement (Hoefel and Elgar, 2003; Almar et al., 2010; Splinter et al., 2011; Walstra et al., 2012; Dubarbier et al., 2015; Fernández-Mora et al., 2015). Both Walstra et al. (2012) and Dubarbier et al. (2015) concluded that more oblique incident waves tend to cause increased offshore sandbar migration under certain wave climates. Regarding the effect of wave angle on bar height changes, Walstra et al. (2012) also found that the oblique incident waves induce bar growth, whereas shore-normal waves tend to cause bar decay. On the other hand, Dubarbier et al. (2015) did not find any significant correlation between wave angle and bar height changes. All the existing beach profile models are site specific and are controlled by a number of calibration parameters that vary from one site to another (Fernández-Mora et al., 2015). These considerable variations in the empirical parameters from one site to another may indicate an attempt of applying constraining parameters to compensate model limitations that primarily arise from simplifications of the physics (Walstra et al., 2012; Dubarbier et al., 2015). Systematic field measurements of sandbar characteristics at a regional scale are therefore crucial to improve our modeling capability.

In this study, beach profiles surveyed every two months along a 15-km stretch of west-central Florida coast over a 4-year period are analyzed to answer the following questions. What are the morphodynamic characteristics of nearshore bars under low wave energy and micro-tidal conditions? More specifically, what is the morphodynamic equilibrium of the sandbar height and cross-shore bar location? How do storm events impact such sandbar equilibrium? The studied coast extends around a broad headland with a shoreline orientation change of 65 degrees. The curved shoreline provides an opportunity to investigate the longshore variations of sandbar responses to incident wave conditions. The sandbar morphodynamics are examined under various incident wave climates including calm summer seasons, relative energetic winter seasons, and tropical storms. Fifty-one beach profiles surveyed every two months along the coast of Sand Key barrier island over a 4-year period from October 2010 to August 2014 are obtained. Data from two of the 4 years, October 2010 to August 2011 and October 2013 to August 2014 are analyzed to investigate equilibrium bar morphology, represented here by sandbar height and cross-shore bar location. Deviations from the sandbar equilibrium state induced by energetic storms, exemplified by a series of strong winter storms in early 2011 and the Tropical Storm (TS) Debby in June 2012, are subsequently studied. The study area is described in Section 2. The methodologies applied in the study are discussed in Section 3. The results are presented in Section 4 and discussed in Section 5, respectively, and conclusions are given in Section 6.

2. Study area

The west-central Florida coast is composed of a chain of barriers islands (Davis and Barnard, 2003). Sand Key, the longest barrier island along this coast, is bounded to the north by Clearwater Pass inlet and to the south by John's Pass. Both inlets are of mixed-energy type with large ebb-tidal deltas (Gibeaut and Davis, 1993). Complex tidal inlet processes have significant influences on beach morphodynamics at the two ends of the barrier island (Roberts and Wang, 2012). The Sand Key

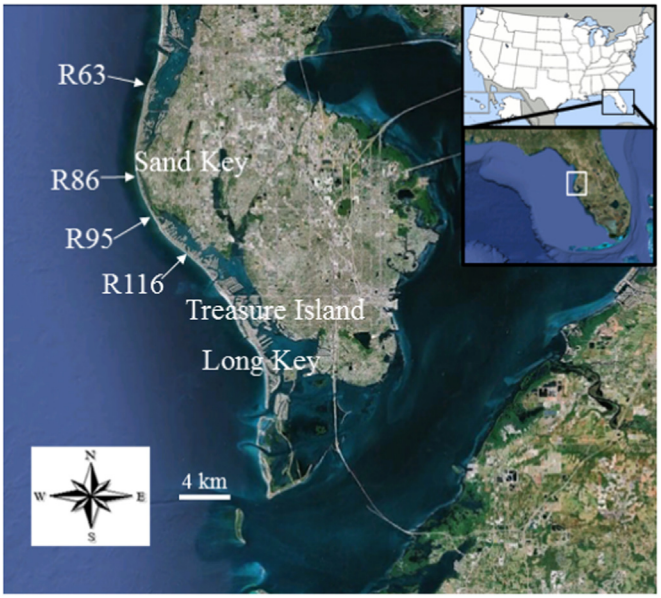

Fig. 1. Study Area: the studied section of beach extends 15 km around a broad headland from R63 to R116 (map source is from Google Earth).

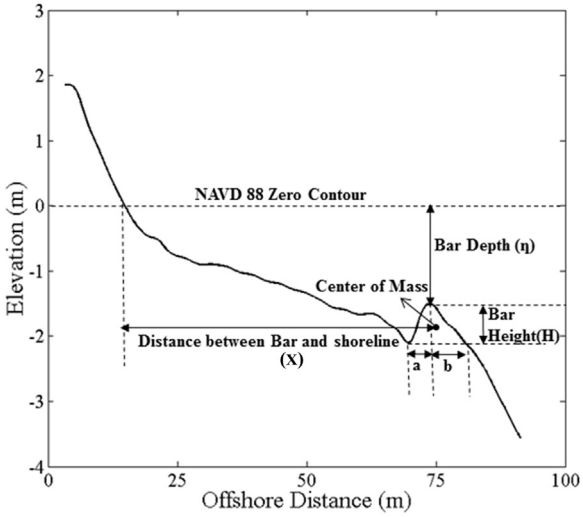

Fig. 2. Definition sketch of bar morphological parameters.

barrier island, extending around a broad headland, has an overall shoreline orientation change of 65° from northwest-facing to southwest-facing beaches, controlled by the antecedent geology (Fig. 1). A large portion of Sand Key has been identified as critically eroding (Florida Department of Environmental Protection, 2011). In order to mitigate the erosion, a long stretch of the beach has been regularly nourished every 6–8 years, the most recent ones being in 2006 and 2012. Sediments along the west-central Florida coast are bimodal composed of siliciclastic and carbonate fractions. The siliciclastic component is primarily fine quartz sand with a mean grain size of roughly 0.16 mm. The carbonate fraction is mostly shell debris of various sizes. Mean grain size in the study area varies typically from 0.15 mm to 1.0 mm, controlled by the varying amounts of shell debris.

The west-central Florida coast has a mixed tide regime, with spring tides being typically diurnal with a roughly 1.0 m range and neap tides being semi-diurnal with a range of about 0.4 m. The wave energy is generally small along the west-central Florida coast, with an averaged nearshore significant wave height of about 0.3 m (Wang and Beck, 2012). Waves are typically sea type generated by local winds. Higher

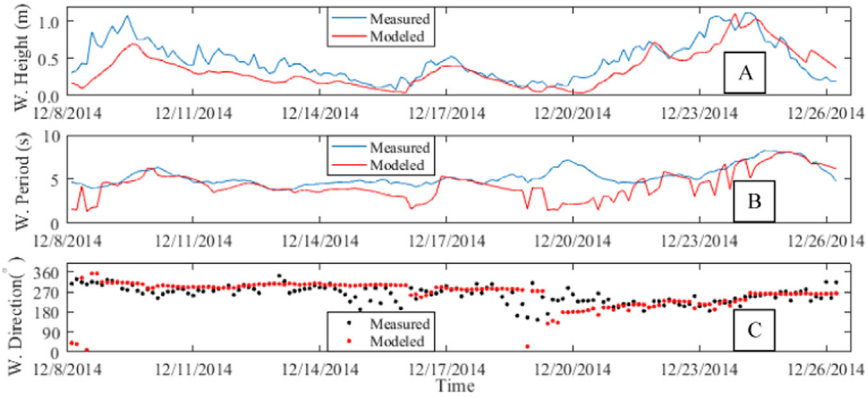

Fig. 3. Comparison between measured wave conditions and calculated wave conditions by WAVEWATCH III: wave height (A), wave period (B) and incident wave angle with respect to North (C).

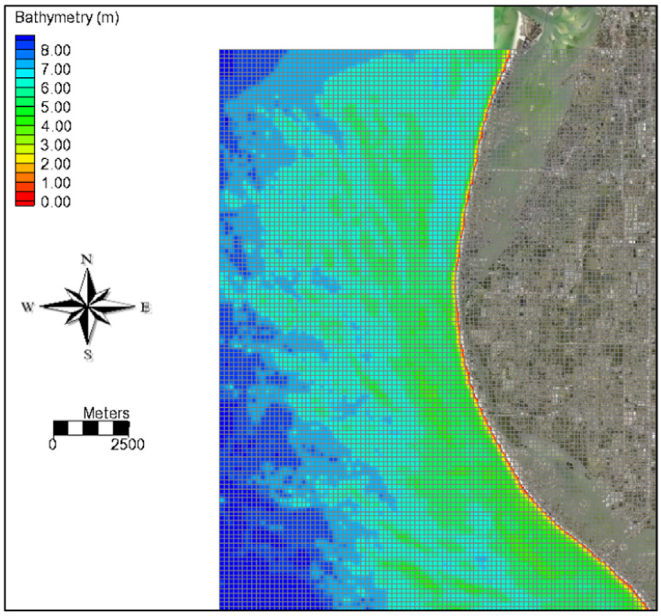

Fig. 4. The grid and bathymetry of CMS-Wave model. The bathymetry is positive downward referred to NAVD 88 zero.

Table 1
Input wave conditions for the CMS-WAVE model.

Time interval	Wave height (m)	Wave period (s)	Wave direction (°)
2 years study period	0.30	4.5	260
October 2010 to Feb 2011	0.40	5.5	290
April 2011 to August 2011	0.17	4.8	200
October 2013 to Feb 2014	0.43	5.0	280
April 2014 to August 2014	0.31	4.0	270
Peak of TS Debby (June 2012 to July 2012)	1.73	9.5	236
Peak of winter storm (Dec 2010 to Feb 2011)	1.86	9.6	272

waves are often associated with the passages of cold fronts every couple of weeks during the winter and occasional passages of tropical storms in the summer. Highly oblique waves generated by the post-frontal northerly winds result in more active southward longshore sediment transport as compared to the northerly transport by the predominant southerly approaching smaller waves. This results in a net annual southward longshore sediment transport (Walton, 1976). It is worth noting that long term (multiple years) beach profile measurements show that the magnitude of beach profile changes along the protruding headland is greater than that of adjacent areas (Wang and Cheng, 2017), indicating the existence of a negative longshore transport gradient due to the shoreline orientation change around the headland.

3. Methods

3.1. Beach profile survey and analysis

From October 2010 to August 2014, a total of 51 beach profiles spaced at about 300 m along the middle section of Sand Key were surveyed every two months. Beach profile shape and temporal changes at the two ends of the barrier island were influenced directly by the tidal inlets and the associated ebb deltas. It is beyond the scope of this paper to examine beach-inlet interactions. Thus the beach profiles from benchmarks R63 to R116 in the middle of the barrier island were investigated in this study (Fig. 1). The survey lines extended from the dune field (or seawall) to about 3 m water depth, or roughly the short-term closure depth in this area (Wang and Davis, 1999). Level-and-transit survey procedures were followed using a Topcon electronic total survey station (Cheng et al., 2016a). The benchmarks established by the Florida Department of Environment Protection along the entire Sand Key shoreline, spaced at 300 m apart, were used. The usually small waves allow the rod-person to hold the rod steady in the water to ensure the accuracy of the survey data. The survey was conducted using NAD83 State Plane (Florida West 0902) coordinate system in meters, referenced to NAVD88 (about 8.2 cm above mean sea level in the study area). The vertical accuracy (including instrumental and operational accuracy) by total station measurement is about ± 2 cm (Lee et al., 2013).

The sandbar characteristics were extracted from the surveyed beach profiles. The bar crests and troughs were identified from the profiles as local points with maximum and minimum elevation, respectively, similar to the procedure used by Ruggiero et al. (2009). Four parameters were defined to represent the morphology of a sandbar (Fig. 2). First, bar height (H) is determined as the elevation difference between sandbar crest and trough. The second parameter is the bar distance, which is computed as the cross-shore position of the center of mass of the sandbar (X, which is the horizontal location of the centroid) with respect to a time-averaged shoreline position (represented here as NAVD88 zero). Notice that the bar distance is referred to a time-independent position. The landward limit of the bar is defined by the location of the trough, while the seaward limit of the bar is defined as the location at the seaward slope of the bar corresponding to the trough level (Fig. 2). As a small bar height tend to yield high uncertainty on the identification of bar location, a threshold of 0.1 m of sandbar height is applied for bar distance computation. The third parameter is bar depth (η), which is the NAVD88 elevation of the bar crest. The fourth

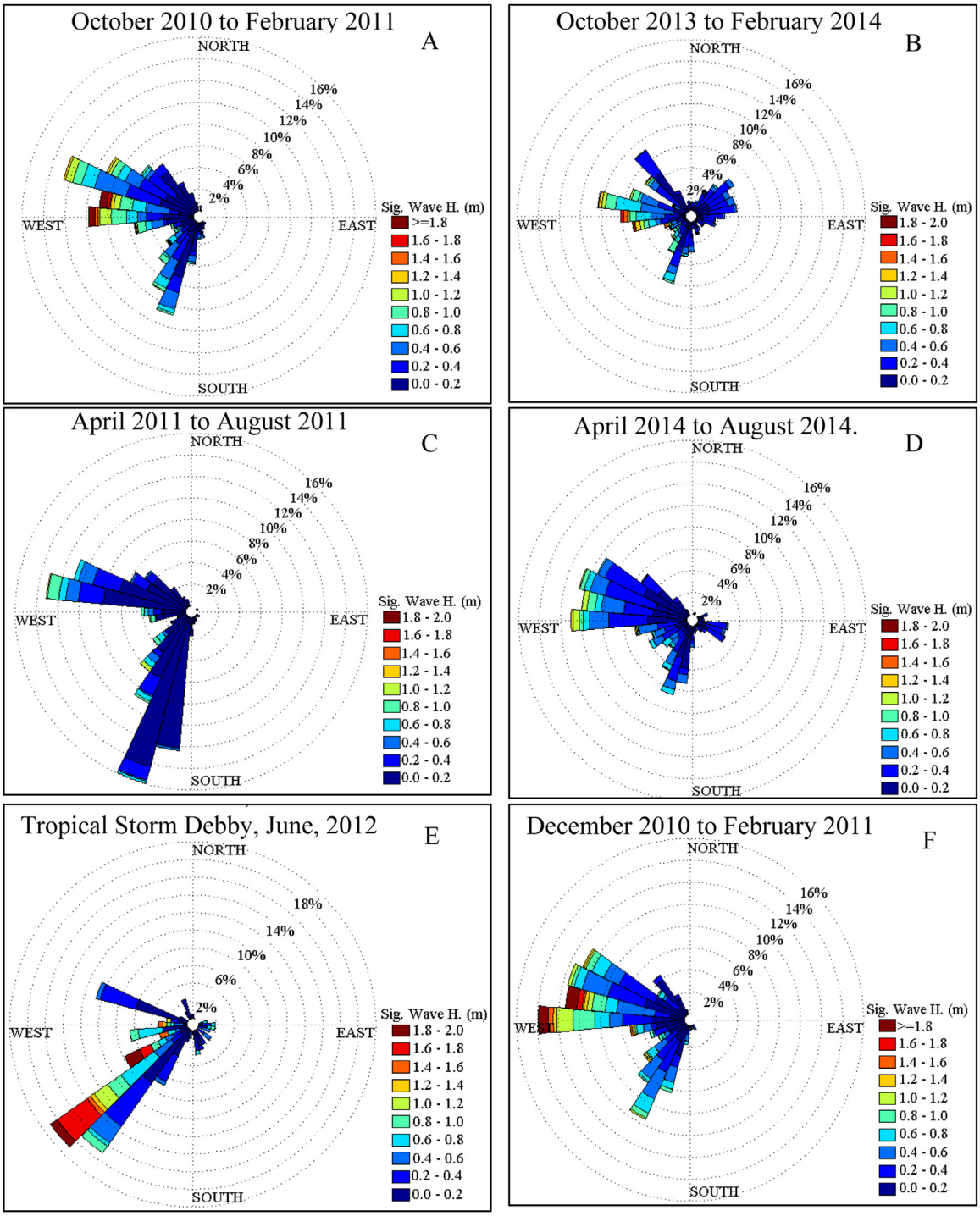

Fig. 5. Offshore wave conditions calculated by WAVEWATCH III: from October 2010 to February 2011 (A), from October 2013 to February 2014 (B), from April 2011 to August 2011 (C), from April 2014 to August 2014 (D), during tropical storm Debby in June 2012 (E), and during a series of winter storms from December 2010 to February 2011 (F).

parameter is sandbar skewness (γ), which can be defined as a/b (Fig. 2) but here we compute it as $\ln(a/b)$ for scaling purposes. Thus a symmetrical sandbar has a skewness value of 0. A negative skewness value indicates a steeper landward slope as compared with the seaward slope, while a positive skewness value represents a bar with a steeper seaward slope.

Shoreline position defined as the intersection between beach profile and NAVD 88 zero was extracted at the seasonal and storm scale to identify the interaction of shoreline changes with sandbar movements. Erosion or deposition over the entire profile was calculated as the volume changes above the short-term depth of closure (DOC) up to the highest elevation of the beach profile to investigate the sediment balance along the studied coast.

3.2. Temporal scale of beach profile analysis

The beach profile analyses were conducted using two temporal scales: seasonal scale and storm scale. Seasonal beach-bar changes were analyzed during two years: October 2010-August 2011 and October 2013-August 2014 in order to obtain the equilibrium bar

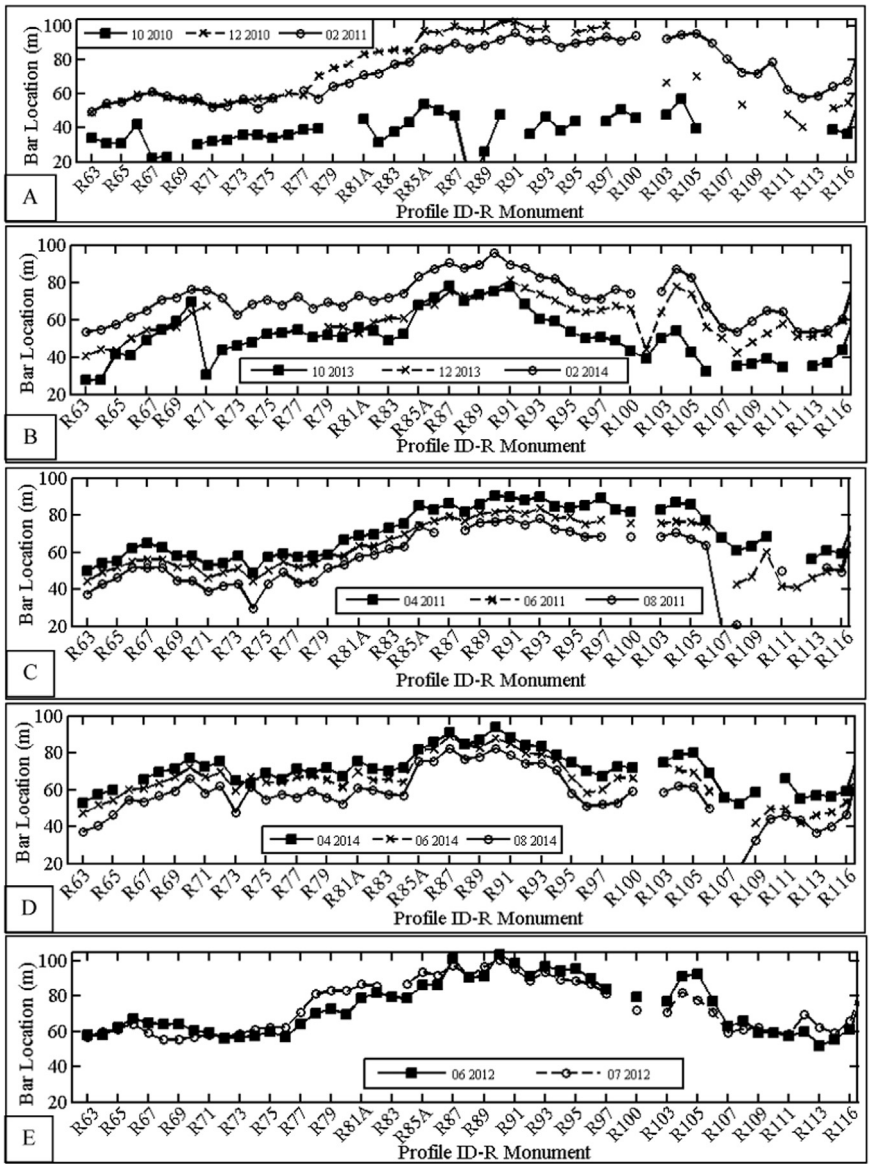

Fig. 6. Temporal and spatial variations of cross-shore bar location (distance between bar and zero NAVD 88): from October 2010 to February 2011 (A), from October 2013 to February 2014 (B), from April 2011 to August 2011 (C), from April 2014 to August 2014 (D), during the tropical storm Debby, 2012 (E).

characteristics. For the study area, October marks the start of the winter season, and August represents the peak of summer season. The equilibrium bar height and equilibrium cross-shore bar location were computed by averaging along the studied temporal domain. The year 2012 was not included in the seasonal analysis due to the occurrence of TS Debby, which is discussed separately at a storm scale. In addition, a beach nourishment project was conducted along the studied shoreline directly after TS Debby in June 2012. As documented by Elko and Wang (2007) and Roberts and Wang (2012), post-nourishment beach profile equilibrium occurred rapidly, dominated by the first energetic post-nourishment storm. Therefore, the influence of the 2012 beach nourishment on the 2013–2014 seasonal changes should not be significant.

The storm scale, as studied here, typically spans one to two months, as determined by the pre- and post-storm survey dates. TS Debby impacted the study area in the early summer of 2012, inducing substantial beach and nearshore bar changes (Cheng and Wang, 2015b). The pre-storm survey was conducted about two weeks before the storm impact and the post-storm survey was conducted one week after. In addition, the beach and sandbar changes induced by a series of winter storms between December 2010 and February 2011 were investigated.

3.3. Hydrodynamic and morphodynamic conditions

As there is no long-term record of measured incident wave conditions in the nearshore area, the wave conditions during the study period were extracted at a numerical station located about 7 km offshore in 8 m water depth from the WAVEWATHCH III model (Tolman, 2014). The WAVEWATCH III modeled wave conditions were compared with waves measured a few km south of the study area from December 8, 2014 to December 26, 2014 (Fig. 3). The 19-day comparison period included the passages of two typical winter cold fronts. Overall, the modeled wave conditions compared reasonably well with the measured data but consistently underestimated the wave height and period. This is likely caused by the fact the computed waves did not fully include the contributions of distal swells. The measured wave height and period are approximately 1.2 times of the modeled values. Thus, the modeled wave height and period are multiplied by 1.2 in the following analyses.

In order to investigate the relationship between the equilibrium bar parameters and incident wave conditions, nearshore wave field along the studied coast was simulated using CMS-WAVE model (Lin et al., 2011). Developed by US Army Corps of Engineering, CMS-Wave is a

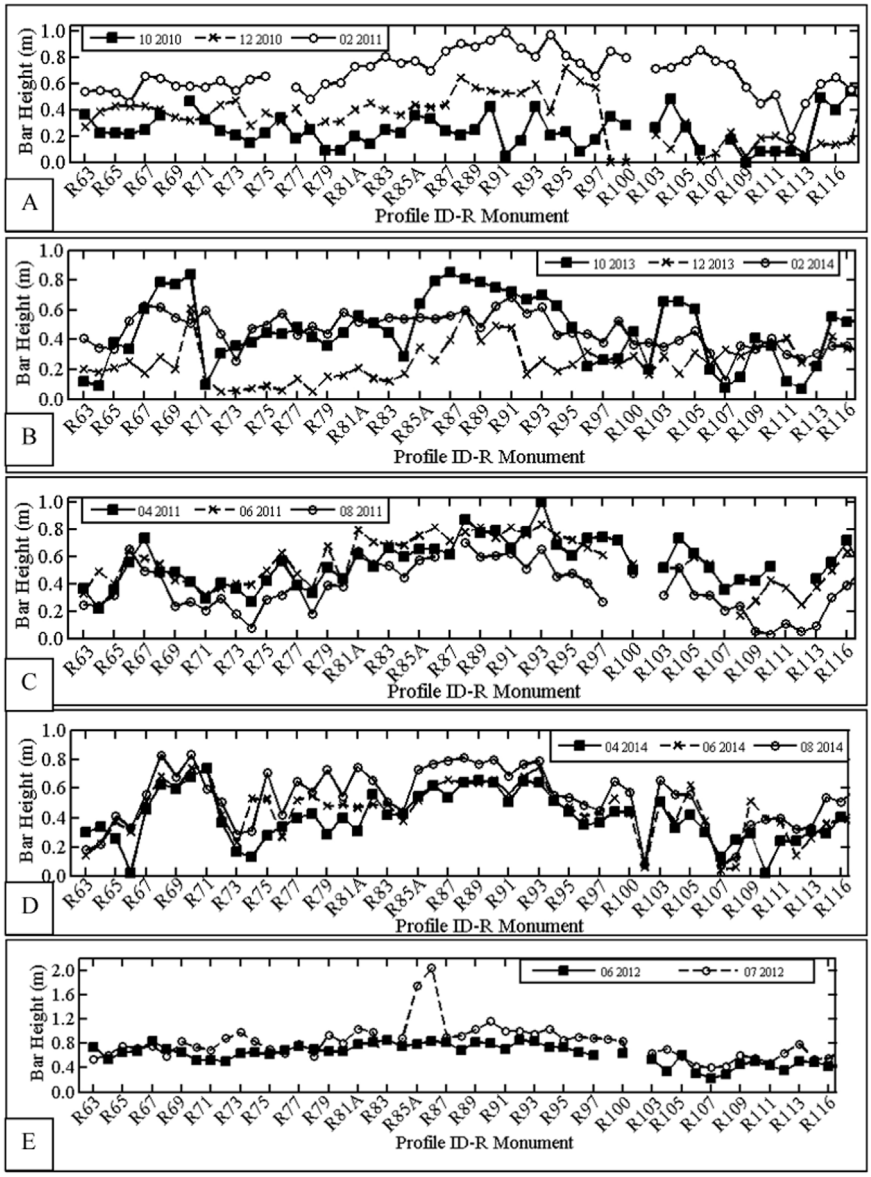

Fig. 7. Changes of bar height: from October 2010 to February 2011 (A), from October 2013 to February 2014 (B), from April 2011 to August 2011 (C), from April 2014 to August 2014 (D), during the Tropical Storm Debby 2012 (E).

Table 2
Summary of alongshore averaged bar-morphology evolution during winter and summer seasons, the dashed line in the middle of the table separate the seasonal and storm scales.

Time period	Movement Distance (m) +: offshore; −: onshore	Height Change (m) +: increase; −: decrease
Oct. 2010 to Feb. 2011	34.9	0.4
Oct. 2013 to Feb. 2014	9.9	− 0.2
Apr. 2011 to Aug. 2011	− 14.2	− 0.2
Apr. 2014 to Aug. 2014	− 14.0	0.1
Jun. 2012 to Jul. 2012	0.2	0.2
Dec. 2010 to Feb. 2011	2.2	0.3

finite-difference, phase-averaged spectral wave model based on the wave action balance equation (Mase, 2001). It employs a forward-marching, finite-difference method to solve the wave action conservation equation for wave transformation including wave shoaling, refraction, diffraction, reflection, and depth-limited breaking (Lin et al., 2011). The CMS-WAVE model has been calibrated and applied in the study area (Wang et al., 2015; Wang and Beck, 2012). A 150 × 150 m model grid was constructed using bathymetric data from NOAA's Coastal Relief Model for the offshore area and bathymetric data collected within this study for the nearshore area (Fig. 4). The latter bathymetric survey was conducted by this study using a synchronized RTK-GPS and a precision echo sounder extending to at least 1000 m seaward from the shoreline. The various input wave conditions applied are listed in Table 1. Time averaged values of wave height and period were computed over different time periods. The modeled wave conditions were extracted at 300 m from the shoreline at the beach profile locations. Finally, a correlation analysis between alongshore variability of wave conditions and sandbar parameters was conducted.

4. Results

4.1. Incident wave characteristics

During the two studied winters (2010–2011 and 2013–2014), cold fronts impacted the study area frequently, every 10–14 days starting mid-October. Fig. 5A and B illustrate the wave conditions during the

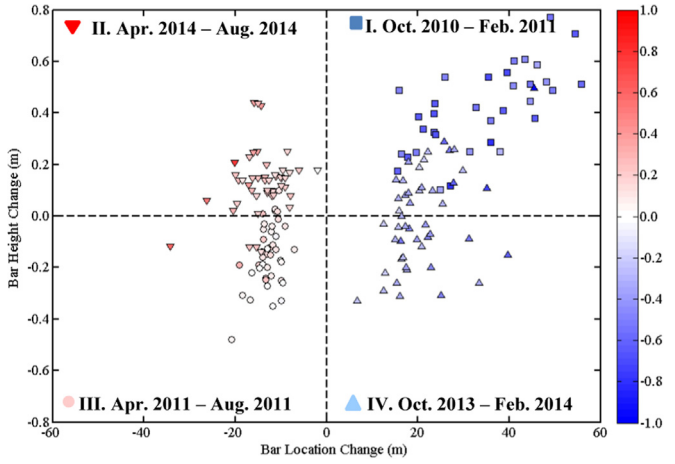

Fig. 8. Bar location change with respect to bar height change at seasonal scale, the colorbar representing the bar crest elevation change. Positive corresponds to values larger than the seasonal values, and negative corresponds to value smaller than the seasonal values. Four types of bar response are included, offshore migration and height increase (I); onshore migration and height increase (II), onshore migration and height decrease (III), and offshore migration and height decrease (IV).

two studied winter seasons from October 2010 to February 2011 and October 2013 to February 2014, respectively. In these periods, waves approached mostly from the west to west-northwest. The summer wave conditions are shown in Fig. 5C–D. Generally, and including the two studied years, the summer waves are considerably lower than those in the winter season. Summer waves tend to approach from south-southwest (Fig. 5C) and west-northwest directions (Fig. 5D).

Fig. 5E illustrates the wave conditions during the passage of TS Debby in June 2012. The majority of the waves approached from the southwest. The peak nearshore wave height during TS Debby reached 2 m. The winter storms studied here approached the coast from west-northwest direction (Fig. 5F). The maximum nearshore wave height is similar to that during TS Debby. In other words, the summer storm examined here (TS Debby) had similar strength than the studied winter storms, i.e. it does not represent extreme conditions that may accompany strong tropical storms.

4.2. Beach and sandbar changes at seasonal scale

Profile data collected from October 2010 to August 2011 and October 2013 to August 2014 were analyzed to examine seasonal variations of bar morphology both alongshore and across-shore. The alongshore distribution of bar position at various times during the study period is illustrated in Fig. 6. The alongshore averaged bar position over the two years during the peak of the winter season (February) and the peak of summer season (August) is 73 m and 57 m, respectively. Overall, a distinctive sandbar typically exists along the coast throughout the studied period. The gaps in the data at the southern end of Sand Key (from R100 to R113) during the survey conducted in October 2010 and February 2011 (Fig. 6A), were caused by the fact that a distinctive bar did not exist at that particular location at that particular time. The alongshore bar positions appear to follow the broad headland. At the apex of the headland, the sandbar is located further offshore as compared to the sandbar locations along the two flanks of the headland (Fig. 6). Although the bar position varied with time, this particular spatial pattern was generally maintained. This suggests that the presence of the headland has an overall control on the bar position.

Offshore-directed sandbar migration occurred during both winter seasons from October 2010 to February 2011 (Fig. 6A), and from October 2013 to February 2014 (Fig. 6B). However, bar-height changes were different during the two periods. The spatially averaged bar height increased during the period from October 2010 to February 2011 (Fig. 7A). In contrast, the bar height mostly decreased during the period from October 2013 to February 2014 (Fig. 7B).

Onshore sandbar migration occurred during both summer seasons from April 2011 to August 2011 (Fig. 6C), and from April 2014 to August 2014 (Fig. 6D). However, the trend of bar-height change was again different. The spatially averaged bar height decreased from April 2011 to August 2011 (Fig. 7C), and increased from April 2014 to August 2014 (Fig. 7D). Thereby, the sandbar height did not demonstrate any apparent seasonal pattern and all four possible combinations of bar height and bar movement trends could be observed, i.e., onshore migration and bar-height increase, onshore migration and bar-height decrease, offshore migration and bar-height increase, and offshore migration and bar-height decrease, occurred during the study period at the seasonal scale (Table 2). The bar-location changes versus bar-height changes over the two winter and summer seasons are shown in Fig. 8. A significant positive correlation between bar-height change and bar-location change exists in quadrants I and III. A linear correlation is not apparent in quadrants II and IV. A possible explanation may be that when the sandbar migrated further offshore more vertical space became available resulting in greater bar height (quadrant I in Fig. 8), while when the bar migrated onshore the vertical space was restricted resulting in shorter bar height (quadrant II in Fig. 8). When the bar moves offshore, the bar crest elevation decreases despite the increase of bar height (quadrant I in Fig. 8), while when the bar moves onshore, the bar crest elevation increases despite the decrease of bar height (quadrant III in Fig. 8). Two representative profiles, one from north of the headland at R77 (Fig. 9A), and one south of the headland at R103 (Fig. 9B), are examined in detail here. Despite the distinct seasonal changes of the nearshore bar morphology described above, the supratidal and intertidal beach remained relatively stable during the different seasons with much smaller magnitudes of changes.

The observed onshore and offshore bar migration pattern characterizes the seasonal cycle of the beach profiles along west-central Florida coast. Similar seasonal patterns have been documented along fetch limited micro-tidal coasts such as along the Mediterranean Sea (King and Williams, 1949; Bowman and Goldsmith, 1983). In contrast with the net offshore migration (NOM) of sandbars that commonly occur at multi-barred beaches along high-energy coasts (Kuriyama et al., 2008; Castelle et al., 2007), the low-energy beach along west central Florida coast does not experience the development of a new bar or the decay of an existing bar. The same sandbar migrates onshore or offshore as controlled by wave conditions. This bar behavior, which does not include a NOM, is again consistent with observations at other low-energy coasts, including beaches at the NW Mediterranean Sea (Ojeda et al., 2011) and stretches of the Dutch coast sheltered with groins (De Schipper et al., 2016).

The alongshore averaged beach volume change landward of the − 3 m contour (or short term depth of closure), summarized in Table 3, is mostly close to zero over the seasonal scales (see also Fig. 10B–D), with the exception of the winter season from October 2010 to February 2011 (Fig. 10A). Shoreline retreat occurred during the winter seasons (Fig. 10A, B, Table 3), while during the typical summer condition the shoreline tended to advance seaward (Fig. 10C, D, Table 3). The overall trend of shoreline change and that of bar-location change at the seasonal scale illustrate a negative correlation during winter and a positive correlation during summer. Although the correlation coefficient is relatively low, the p value (mostly less than 0.05) suggests that the correlation is significant (Fig. 11). This suggests that, during the winter time, landward shoreline movement is associated with seaward movement of sandbar. In contrast, during the summer time, seaward movement of shoreline tends to be associated with landward migration of sandbar. This negative correlation between shoreline and sandbar location was also observed at La Barceloneta beach, located at the low-energy NW Mediterranean Sea (Ojeda et al., 2011).

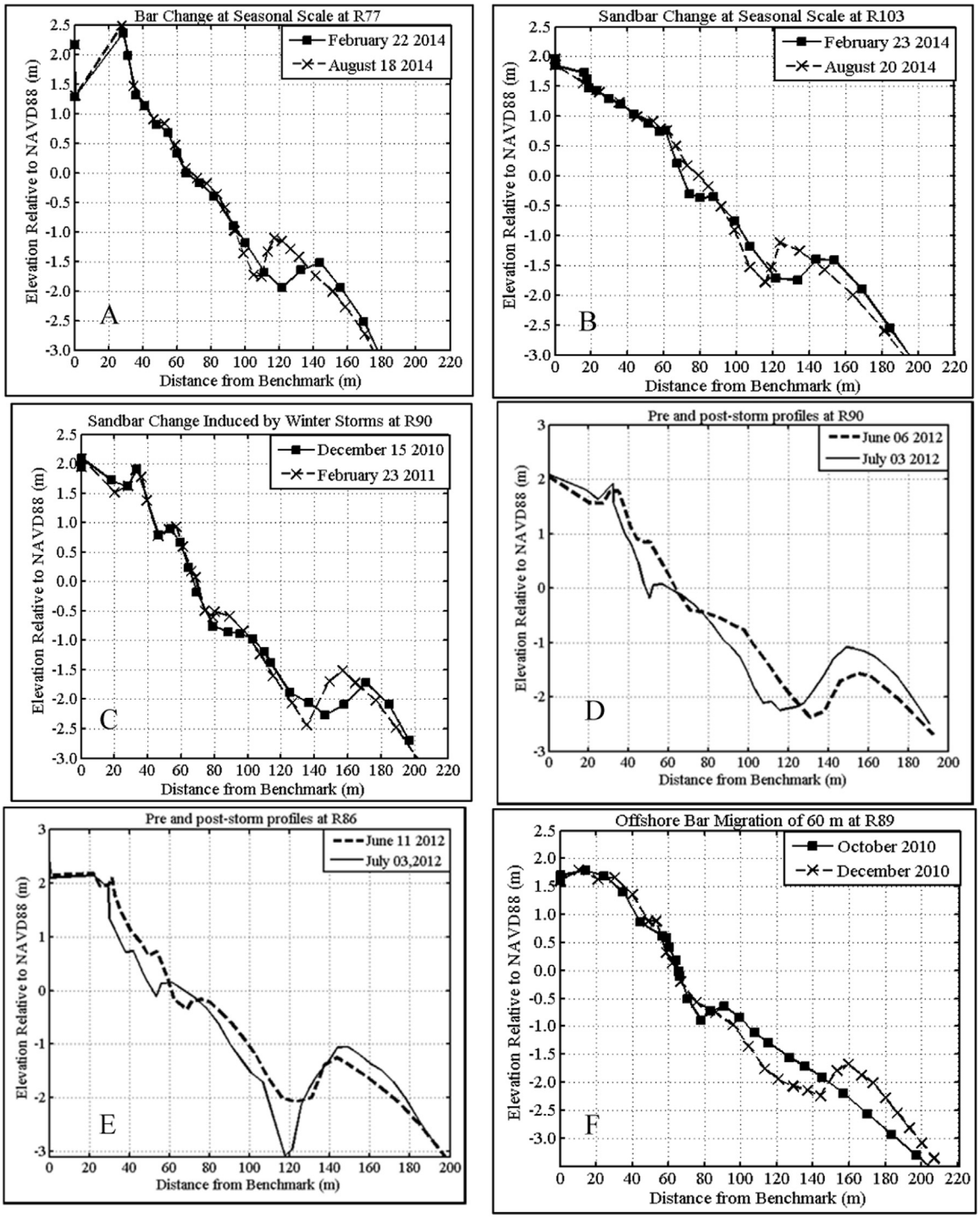

Fig. 9. Examples of sandbar-beach profile changes at: R77 at seasonal scale (A), R103 at seasonal scale (B), R90 at storm scale (C), R79 at storm scale (D), R86 at storm scale (E), R89 with bar migration of 60 m due to winter storms (F).

4.3. Beach and sandbar changes at storm scale

For the storm scale study, profile changes associated with TS Debby in 2012 and a series of winter storms from December 2010 to February 2011 were analyzed. The general winter-summer seasonal pattern discussed in the previous section can be disrupted by individual storms. For example, onshore bar migration, as opposed to offshore migration, was measured at some profile locations (e.g. at R90) after a series of winter storms (Fig. 9C). While apparent sandbar upward aggradation was measured at R90 (bar remained mostly at the same cross-shore location with significant bar height increase) during TS Debby in 2012 (Fig. 9D). However, the above bar-position change during individual storm at some profiles locations did not alter the overall seasonal pattern as described above (Fig. 9A, B). At some profiles, a deep scour hole occurred during the storms, considerably increasing the bar height (Fig. 9E). A seaward sandbar migration of up to 60 m was measured during October to December 2010 at some locations (Fig. 9F), which represent the maximum distance of sandbar movement over the study period. A seaward sandbar migration of about 70 m was also measured at a low-energy beach during a winter storm (Ojeda et al., 2011).

Table 3
Alongshore averaged beach volume change above short term depth of closure and shoreline changes.

Time Interval	Beach volume change m^3/m	Shoreline change (m)
October 2010 to February 2011	− 9.24	− 1.09
April 2011 to August 2011	1.92	0.84
October 2013 to February 2014	− 3.32	− 3.2
April 2014 to August 2014	1.34	0.28
TS Debby (June 2012)	1.5	− 3.87
December 2010 to February 2011	− 5.32	1.55

Considerable alongshore variation of sandbar movement was observed during the two storm events. During the peak winter season between December 2010 to February 2011, alongshore variation of bar movement was measured: onshore migration occurred at most profiles from R79 to R97, while offshore bar migration occurred at most profiles located between R103 and R116 (Fig. 6A). Alongshore variations of bar movement were also measured during the studied summer storm TS Debby 2012 (Fig. 6E): offshore sandbar migration occurred at most profile locations north of the headland (From R76 to R87), while south of the headland onshore sandbar migration was measured at most profiles (from R93 to R107) (Fig. 6E). At the headland (from R88 to R92), the sandbars tended to stay at similar location but grew higher (Figs. 6E, 7E).

The alongshore averaged beach volume change landward of the − 3 m contour (or short term depth of closure) is also close to zero over the TS Debby (Fig. 10E, Table 3). During the impact of TS Debby, substantial shoreline retreat occurred (Fig. 10E), while the changes of beach-volume above the − 3 m contour do not correspond to the negative shoreline-change trend. This suggests that the net sediment transport is dominantly in the offshore direction from the dry beach to the subaqueous sandbar. Although the shoreline (NAVD88 0 m contour) advanced seaward during the series of winter storm from December 2010 to February 2011 (Fig. 10F), substantial erosion occurred on the

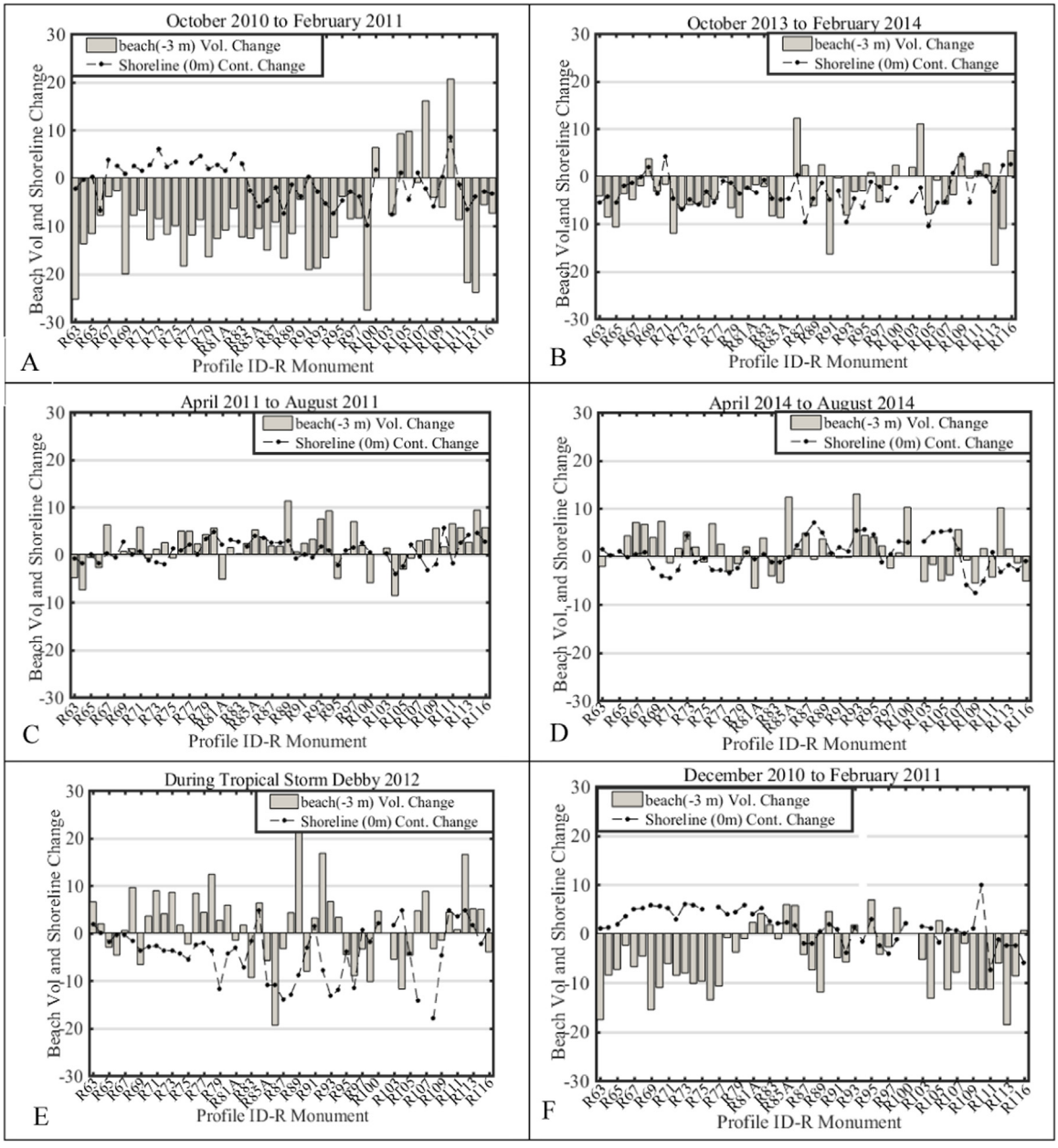

Fig. 10. Volume and shoreline (NAVD88 0 m contour) change from October 2010 to February 2011 (A); from October 2013 to February 2014 (B); from April 2011 to August 2011 (C); from April 2014 to August 2014 (D); During the Tropical Storm Debby, 2012 (E) Winter storms during Dec. 2010 to Feb. 2011 (F).

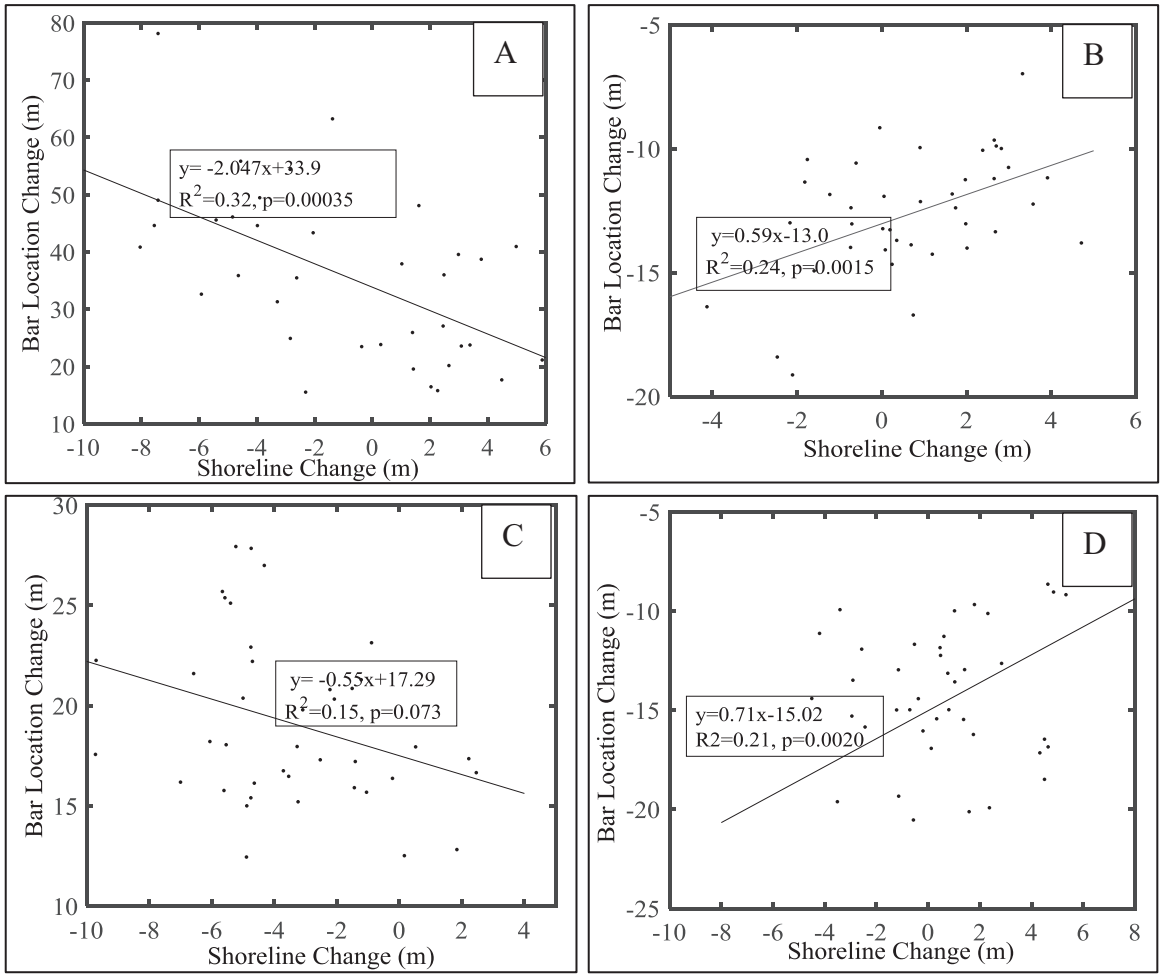

Fig. 11. Linear relationship between shoreline change and bar location change: from October 2010 to February 2011 (A); from April 2011 to August 2011 (B); from October 2013 to February 2014 (C); from April 2014 to August 2014 (D).

dry beach and in the dune field (NAVD88 1 m contour and above).

4.4. Sandbar skewness

The sandbar skewness was closely related to the direction of bar movement, with the winter sandbar having substantially greater skewness values ($\ln(a/b)$) than those of summer sandbars (Fig. 12A and B). The skewness values of the winter sandbar were mostly positive (offshore skewed), with an averaged value of 0.15, while the skewness values of the summer sandbar were mostly negative (onshore skewed), with an averaged value of -0.5.

Based on prototype-scale laboratory data, Cheng et al. (2016b) found that symmetrical bar shape was maintained when the beach profile reached an equilibrium state. The seasonal bar skewness variation between positive and negative, as shown in Fig. 12, suggests that sandbar equilibrium is dynamic, maintained via constant onshore and offshore migrations. In general, during the summer season the sandbar is typically skewed with a steep landward slope in agreement with its onshore migrating trend, while during the winter season the sandbar tend to be skewed with a steeper seaward slope corresponding to a seaward migrating trend.

5. Discussion

5.1. Effect of wave height on the alongshore variation of the sandbar

The causes of longshore variations of sandbar configurations are discussed here. The time-averaged bar height and cross-shore bar location during the 2-year study period were calculated along the studied coast. The values should represent the dynamic equilibrium bar parameters (Fig. 13A). Along the 15-km studied coastline, the equilibrium (average) bar height ranged from approximately 0.20 m to 0.70 m, with greater equilibrium bar height around the headland and lower height along the two flanks. The equilibrium (average) bar distance ranges from about 40–80 m from the shoreline, also with a greater distance around the headland (Fig. 13A). A linear correlation exists between the bar height and cross-shore bar location (Fig. 13B). As discussed in Section 4.2, the bar associated with the headland tend to have greater bar height and be located further offshore.

Nearshore wave height distribution was modeled using the CMS-WAVE model under the average wave condition over the 2-year study period (Table 1, Fig. 14A). A highly significant linear correlation exists between alongshore variation of bar heights and wave heights (Fig. 15A). This indicates that greater wave height yields greater equilibrium bar height, although a considerable degree of scattering exists. It is worth noting that, the correlation between bar height and bar position, as discussed in Section 4.2, suggest that bar position also correlates with wave height.

The wave field was also modeled under the studied two summer seasons, two winter seasons, and two storm conditions, and four of these six cases are shown in Fig. 14. Under the majority of the circumstances, the highest wave occurs around the headland, with a secondary peak along the northern flank of Sand Key. Significant linear correlation exists between wave height and bar height for the four cases

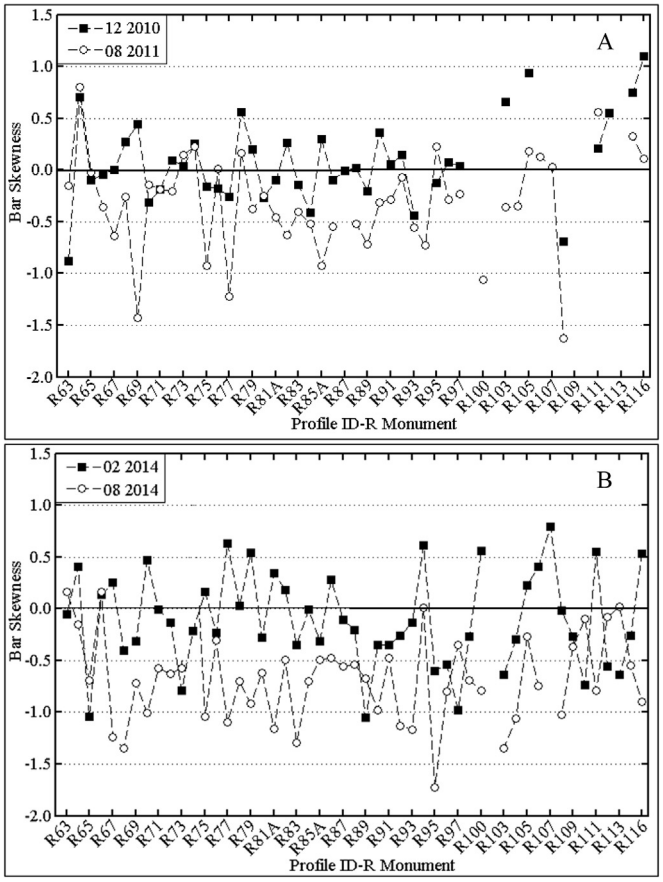

Fig. 12. Bar skewness, ln(a/b), during the winter and summer seasons from December 2010 to August 2011 (A) and from February 2014 to August 2014 (B).

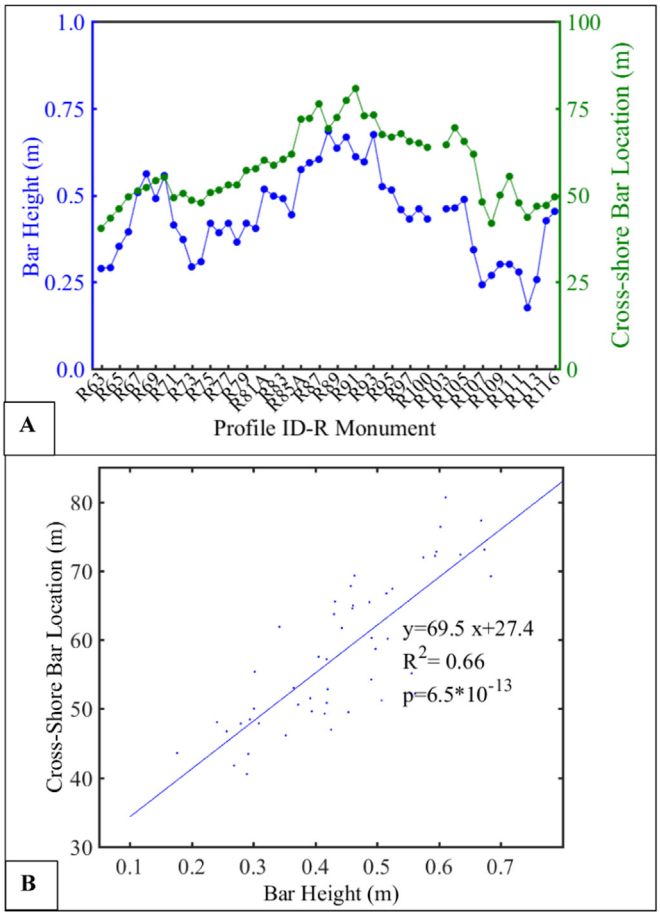

Fig. 13. Equilibrium bar height and cross-shore bar location along the studied coast (A); correlation between the equilibrium bar height and cross-shore bar location (B).

(Fig. 15). However, for the winter season from October 2010 to February 2011 and the winter storm period from December 2010 to February 2011, no significant linear relationship was identified. These two cases are not shown in Figs. 14 and 15. Based on field observations of sandbar behavior along a curved coast, Rutten et al. (2017) also found that longshore variations of sandbar configuration are related to alongshore difference in breaker height due to wave refraction. The relationship between bar height and wave height also seems to hold, at least qualitatively, when compared to other high wave-energy sites. For example, along the Duck beach, North Carolina, the 1.1 m averaged wave height corresponds to a 0.9 m bar height (Larson and Kraus, 1994). Along the Long Beach, southwest Washington coast, higher wave yields an averaged bar height of 1.3 m (Leonardo and Ruggiero, 2015).

5.2. Effect of wave angle on the alongshore variation of the sandbar

Numerical modeling of sandbar evolution suggests that incident wave height, angle, and original sandbar crest elevation are the main factors controlling the variations in bar height and cross-shore location (Walstra et al., 2012; Dubarbier et al., 2015). As our study area encompasses a 60-degree shoreline orientation change around a broad headland, it provides an opportunity to investigate the effect of incident wave angle on sandbar morphodynamics. Fig. 16A summarizes the range of hydrodynamic and morphodynamic conditions that are covered by this study for the 51 beach-bar profiles during two winter seasons, two summer seasons, and two storm conditions. Overall, this study encompasses a wide range of incident wave angle (from shore normal to over 70° angle), wave height (from 0.1 m to 1.8), and bar crest elevation (−0.50 m to −1.75 m).

In order to focus on investigating the influence of wave angles on the sandbar morphodynamics, K-mean clustering (Hardle and Simar, 2003) was conducted to generate eight different clusters of bar-crest elevation and wave height combinations (Fig. 16B). Within the same cluster, the variables bar-crest elevation and wave height have the nearest mean (i.e. the averaged distance between the centroid and each point reaches the minimum sum of squared error). In other words, the difference in bar-crest elevation and wave height are mostly eliminated through the clustering. The sandbar variations are, therefore, mostly induced by the varying incident wave angles within the same cluster. For each of the eight clusters, correlation analysis between incident wave angle and sandbar height change, as well as incident wave angle and sandbar distance change were conducted. The bar-height change and incident wave angle does not show significant correlation for none of the 8 clusters. This is consistent with the modeling results from Dubarbier et al. (2015) suggesting the wave angle does not have significant influence on the bar-height variation. Significant correlation between incident wave angle and sandbar migration exists only for cluster #8 and #6 (Fig. 16C, E). For cluster #8, the larger the incident wave angle, the greater the offshore migration of the sandbar (Fig. 16C). A negative correlation between the wave height and wave angle suggests that more oblique wave angle tends to be associated with lower wave height (Fig. 16D). For Cluster #6, smaller incident wave angle appears to be associated with greater onshore sandbar migration (Fig. 16E), with larger incident wave angle also corresponding to smaller wave heights (Fig. 16F).

This above analyses are consistent with the numerical modeling results which suggest that longshore sediment transport induced by

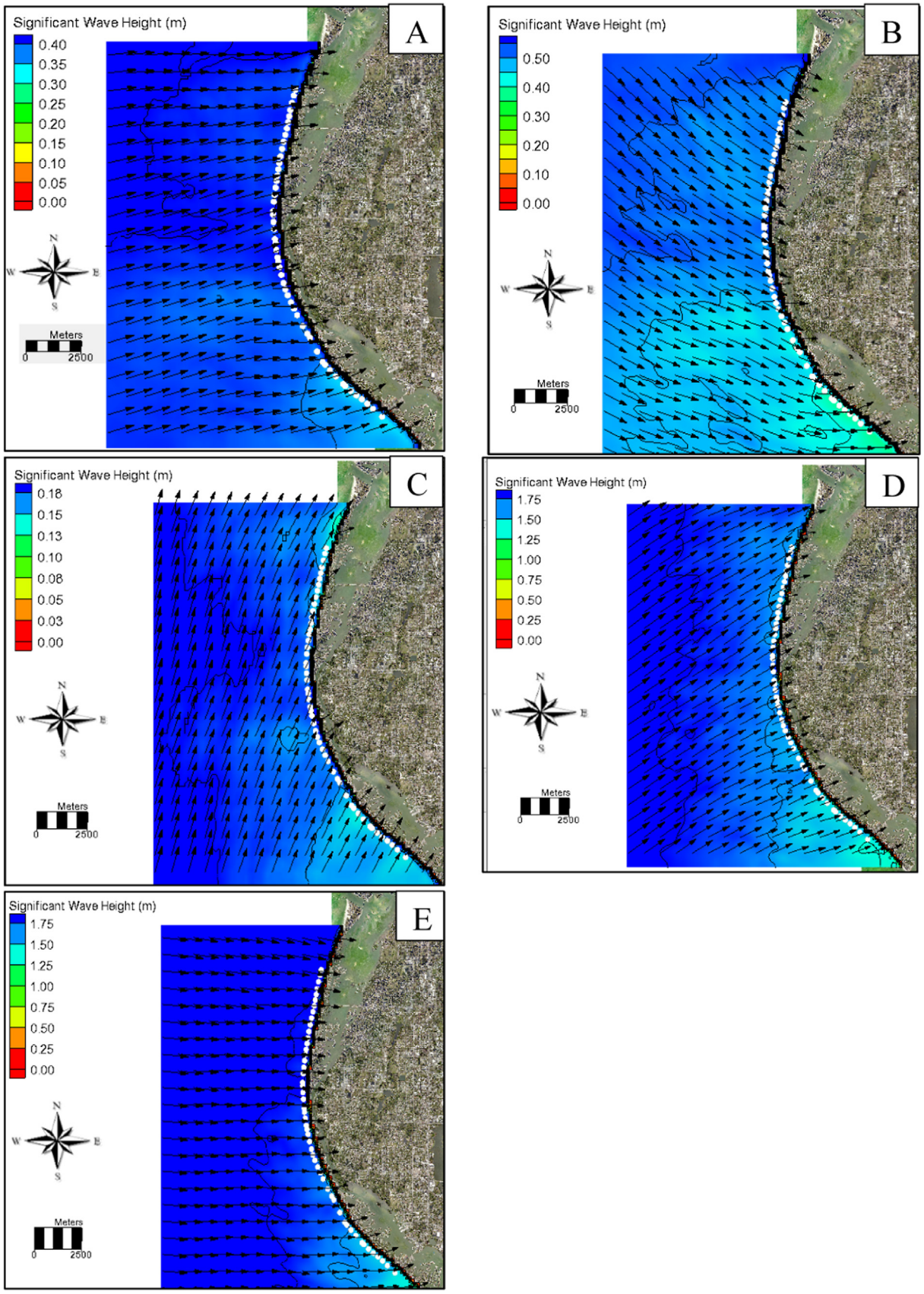

Fig. 14. Simulated wave propagation under averaged conditions: over the 2-year period of seasonal analysis (A); October 2010 to February 2011 (B); April 2011 to August 2011 (C), TS Debby from June 2012 to July 2012 (D); a series of winter storm from December 2010 to February 2011 (E). White dots indicate the locations where computed wave heights were extracted from the model.

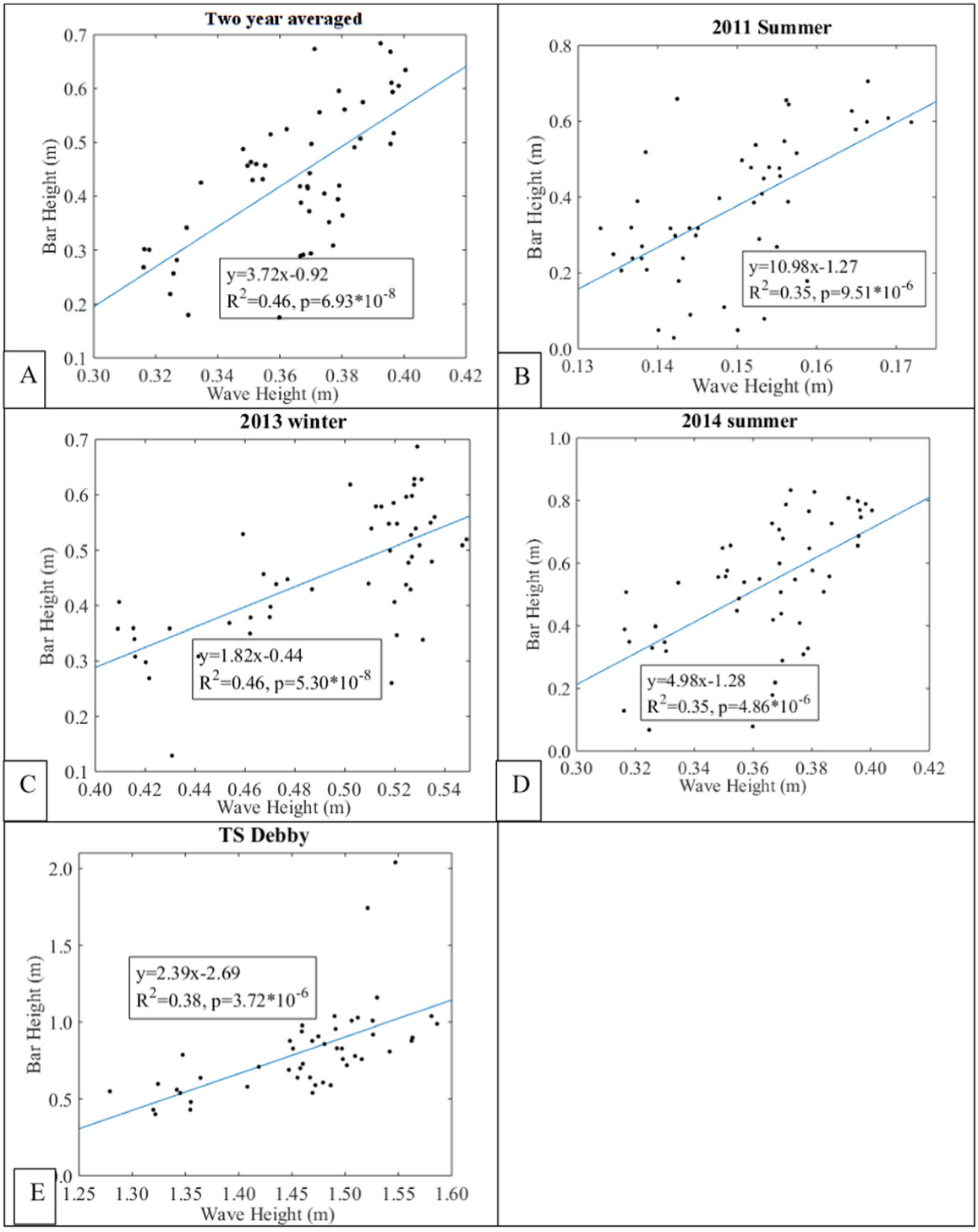

Fig. 15. Correlation between wave height and sandbar height over the 2-year period of seasonal analysis (A), over the period April 2011to August 2011 (B), October 2013 to February 2014 (C), April 2014 to August 2014 (D), the TS Debby (E).

oblique incident waves can cause sandbar to move offshore under certain wave climates (Ruessink and Kuriyama, 2008; Walstra et al., 2012; Dubarbier et al., 2015). One of the main assumptions associated with beach profile models is alongshore uniformity. Although field measurements have demonstrated substantial longshore variations, existing beach-profile models have largely ignored the influence of longshore bathymetry variations (Fernández-Mora et al., 2015). The calibration of beach-profile models is typically conducted at a single location.

5.3. Influence of pre-storm sandbar crest elevation on bar movement

Sandbar crest elevation plays an important role in controlling the direction of sandbar movement (Walstra et al., 2012). The considerable alongshore variation of sandbar movement observed at the storm scale by this study provides an opportunity to investigate the relationship between pre-storm sandbar crest elevation and the subsequent sandbar movement.

The sandbar typically moved offshore south of the headland (from R110 to R116) during the series of winter storms from December 2010

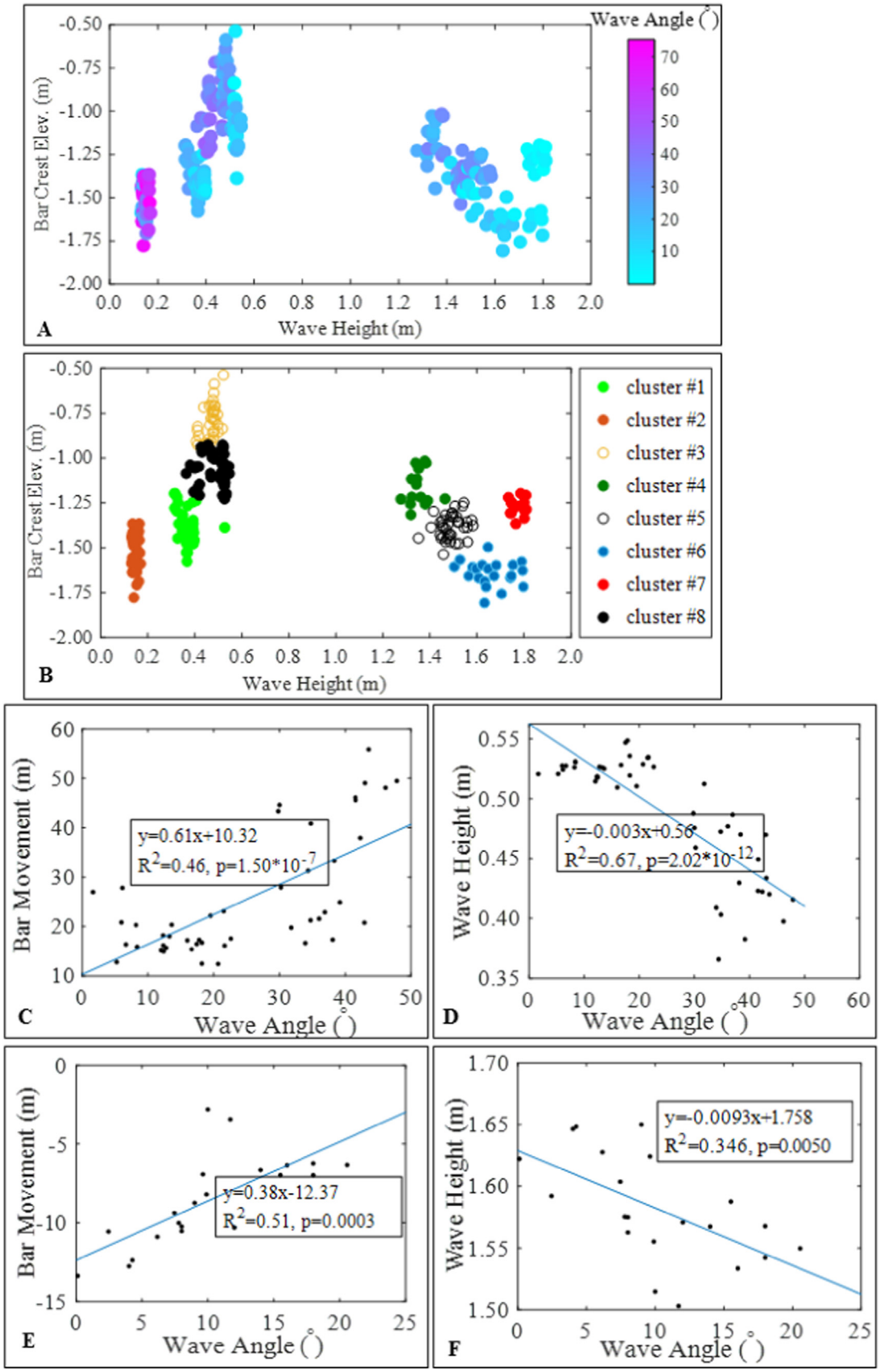

Fig. 16. The range of investigated parameters influencing sandbar morphodynamics (A), eight different clusters of wave height and bar crest elevations (B), incident wave angle versus bar-migration distance for cluster #8(C) and for cluster #6 (E), incident wave angle versus wave height for cluster #8 (D) and for cluster #6 (F).

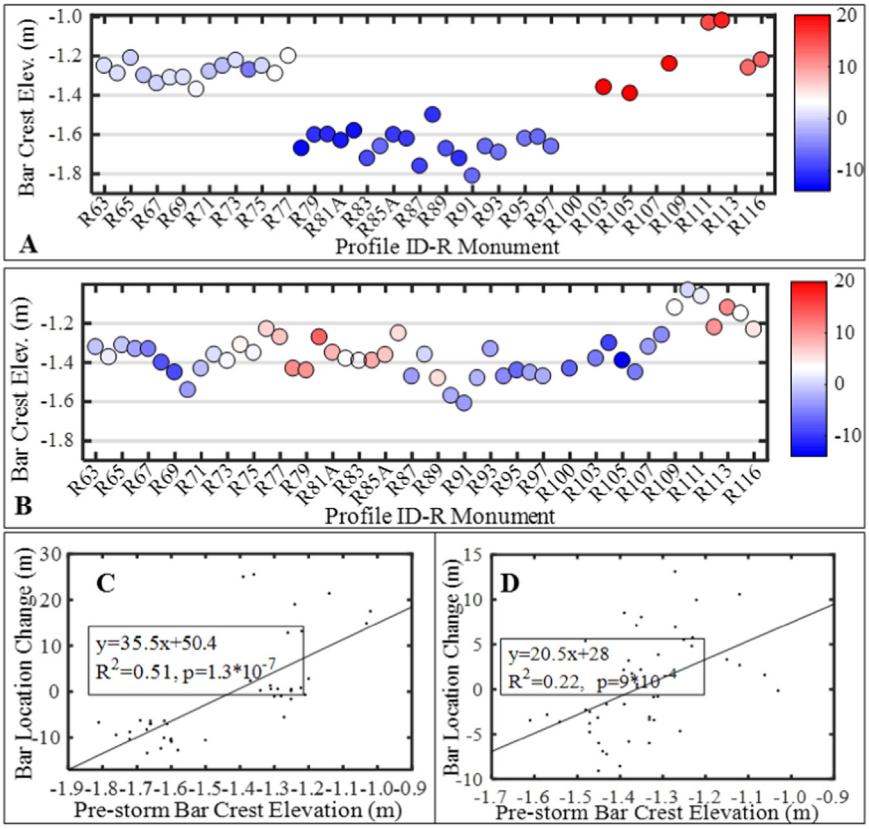

Fig. 17. Pre-storm bar crest elevation relative to NAVD 88 for 2010 winter storms (A), and Tropical Storm Debby in June 2012 (B). The color code represents distance of sandbar migration. Negative value indicates onshore sandbar movement, positive value indicates offshore sandbar movement. Relationship between pre-storm bar crest elevation and bar-location change during the 2010 winter storm (C), and during Tropical Storm Debby (D).

to February 2011 (Fig. 6A). The crest elevation of the pre-storm sandbar for the offshore migrating cases was relatively high (Fig. 17A), i.e., the water depth over the sandbars was small. For the onshore migrating cases at most of the profiles (from R77 to R97) north of the headland (Fig. 6A), the crest elevation of the pre-storm sandbars was relatively low (Fig. 17A), i.e., the water depth over the sandbars was large. Similarly, during the TS Debby, offshore migration occurred (Fig. 6E) when the crest of the pre-storm sandbars was shallower (from R109 to R116 and from R73 to R86) while onshore migration (Fig. 6E) corresponded to a deeper pre-storm bar (at the rest of the profiles) (Fig. 17B). There is a linear relationship between bar movement distance and bar-crest elevation (Fig. 17C, D). Student *t*-test suggested a statistically significant correlation between the above two quantities, since the *p* value is considerably smaller than 0.05. On average, the water depth over the pre-storm sandbars crest for the onshore migration cases was approximately 20 cm deeper than that for offshore migration case. It is worth noting that the accuracy of the total station survey is ± 1.2 cm (Lee et al., 2013), which is one order of magnitude smaller than the 20 cm bar elevation difference. Thus potential survey errors should not have fundamental influence on these findings.

The above relationship between sandbar crest elevation and its onshore-offshore trend of migration may be explained by water-depth control on wave breaking. A shallower sandbar crest would lead to more intense wave breaking over the bar and subsequently more active suspended-load sediment transport, which seems to result in offshore bar migration. On the other hand, a deeper sandbar crest is less efficient in inducing wave breaking and subsequently resulting in less active suspended-load transport and relatively more active bedload transport, which seems to result in onshore bar migration. Numerical modeling also suggested that offshore bar migration is related to a dominance of suspended load transport, while onshore bar migration is dominated by bedload transport (Walstra et al., 2012). This is qualitatively consistent with the above interpretation. Therefore, the initial beach-profile characteristics, particularly the water depth over the sandbar crest, play an important role in controlling the onshore and offshore sandbar movement.

5.4. Storm-induced perturbation to sandbar height

Energetic storms can introduce significant perturbation to the seasonal patterns of sandbar-height and position changes. Almost all the bar heights before TS Debby along the study area were greater than the equilibrium bar height, with an alongshore averaged value of 0.62 m versus an equilibrium height of 0.44 m (Fig. 7E, Fig. 13A). The sandbar height did not decrease and approach to the equilibrium height during the storm impact. Instead, the sandbar became even higher than the pre-storm bar, with an alongshore averaged value of 0.80 m (Fig. 7E). Similarly, for the series of winter storms from December 2010 to February 2011, the sandbar became higher than the pre-storm bar height regardless of the initial height being greater or less than the equilibrium bar height.

The post-storm bar height increase can be attributed to the scour in the nearshore-trough area in combination with deposition over the bar crest, as illustrated in Fig. 9 E. This is an example of a rather extreme case. Most of the profiles demonstrated the trend shown in Fig. 9D, i.e., the pre-storm trough became deeper while the bar crest became higher, resulting in a greater bar height. The high waves associated with an energetic storm caused a perturbation in the seasonal cycle by scouring the nearshore-trough region, which was also observed during large scale laboratory experiments (Wang et al., 2003). Elevated longshore sediment transport rate around the headland may enhance the formation of the scour hole. A deep scour hole was generated by the storm at profiles R85A and R86, at the apex of the headland (Fig. 9E), where the incident wave was the highest along the studied coast (Fig. 14). It is worth noting that erosion was also measured on the dry beach and in the intertidal zone, further contributing to the deposition over the nearshore bar. Considerable deepening of the trough was also observed at a micro-tidal beach along the coast of Sete, France under severe

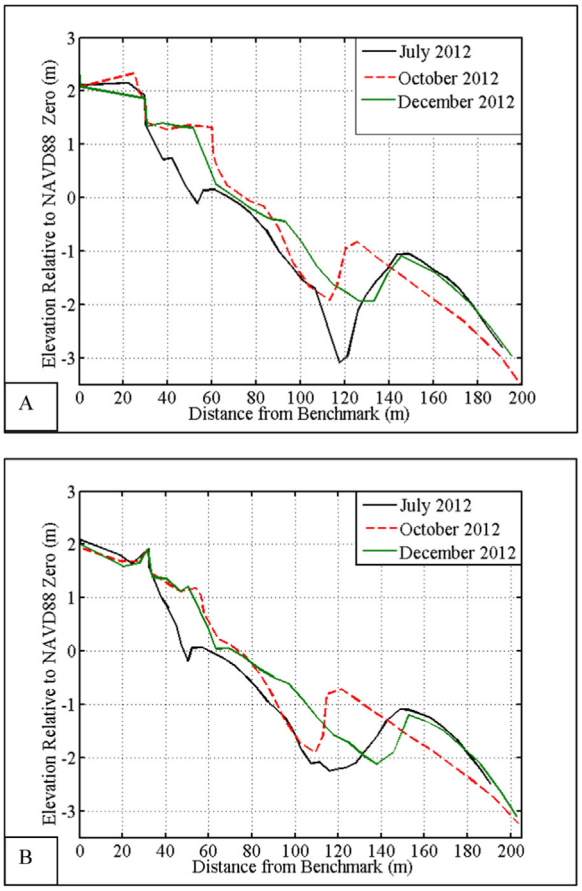

Fig. 18. Post-storm (TS Debby) beach-profile evolution toward equilibrium bar height at profiles R86(A) and R90 (B). The wide beach above NAVD88 zero reflected the beach nourishment.

storm conditions (Certain and Barusseau, 2005). After TS Debby, the higher (and hence shallower) bar experienced substantial erosion as the sandbars migrated onshore during the summer season. The eroded sand from the bar crest was deposited in the trough landward. This resulted in a lower bar height, returning to the dynamic equilibrium height, 4–6 months after the storm impacts, as illustrated in Fig. 18. This demonstrates the equilibrium processes by which the perturbation induced by the energetic storm was absorbed by the seasonal cycle. It should be pointed out that the 2012 beach nourishment project was constructed directly after the impact of TS Debby. The beach fill is apparent on the post-Debby profiles (Fig. 18A, B). However, the nourishment did not fundamentally change the seasonal sandbar pattern, as evident by comparing Fig. 18A and B including a nourishment with panels without nourishment (Fig. 9D and E).

6. Conclusions

A dynamic equilibrium cross-shore sandbar location from the shoreline and bar height have been identified along the curved west-central Florida coast, with values ranging from 40 m to 80 m and 0.20–0.70 m, respectively. The alongshore variation of the equilibrium bar location and height correlate with the alongshore variation in wave height, with the higher bar being further offshore displaced when the wave height is larger, and vice versa.

The sandbar tends to evolve toward this equilibrium position during the seasonal cycle.

The sandbar generally moves onshore during the summer season and offshore during the winter season, with alongshore averaged bar location during the winter and summer being 73 m and 57 m, respectively. Linear correlation exists between wave angle and trend of sandbar movement under certain wave condition. More oblique incident waves tend to induce farther offshore bar migration. In contrast, the sandbar height does not demonstrate an apparent seasonal patterns, as it increases or decreases over the same season. There is no significant linear correlation between incident wave angle and sandbar height changes. The general trend of sandbar height change appears to be controlled by the initial bar height in relation to the equilibrium height. If the initial bar height is greater than its equilibrium value, the bar tends to be eroded. If the initial bar height is smaller than the equilibrium value, the bar tends to grow taller. This explained the different bar-height evolution trends observed during the study period. The dynamic equilibrium bar height can also be used to explain the spatial variation of bar growth (height increase) or decay (height decrease) along the 15-km studied coast at both seasonal and storm scales.

The energetic conditions associated with TS Debby in 2012, as well as the series of winter storms from December 2010 to February 2011, can cause both onshore and offshore migration of the sandbar at different alongshore positions. The water depth over the pre-storm sandbar crest appears to be a key factor influencing the direction of sandbar movement. The offshore migrating sandbar tends to have a shallower pre-storm bar crest, while the onshore moving sandbar tends to have a deeper pre-storm bar crest. These storms also cause a deviation from the dynamic sandbar height equilibrium. Sandbar at most of the profile locations become higher than the pre-storm bar height. However, the sandbar returns to its equilibrium height 4–6 months after the storm impacts.

Sandbar skewness provides an indicator for the direction of bar migration. A steeper landward slope and a gentler seaward slope correspond to a trend of onshore migration, while a steeper seaward slope and a gentler landward slope are associated with an offshore migrating bar.

Acknowledgements

This study was funded by Pinellas County, Florida Grant number 1225111200 and the University of South Florida. Numerous graduate and undergraduate students assisted in field data collection. Two anonymous reviewers are particularly appreciated for their constructive comments and suggestions, which are crucial for an improvement to the original manuscript.

References

Aleman, N., Robin, N., Certain, R., Anthony, E.J., Barusseau, J.P., 2015. Longshore variability of beach states and bar types in a microtidal, storm-influenced, low-energy environment. Geomorphology 241, 175–191.
Almar, R., Castelle, B., Ruessink, B.G., Senechal, N., Bonneton, P., Marieu, V., 2010. Two- and three-dimensional double-sandbar system behaviour under intense wave forcing and a meso-macro tidal range. Cont. Shelf Res. 30, 781–792.
Browder, A.E., Dean, R.G., 2000. Monitoring and comparison to predictive models of the Perdido Key beach nourishment project, Florida, USA. Coast. Eng. 29, 173–191.
Brutsché, K.E., Wang, P., Beck, T.M., Rosati, J.D., Legault, K.R., 2014. Morphological evolution of a submerged artificial nearshore berm along a low-wave microtidal coast, Fort Myers beach, west-central Florida, USA. Coast. Eng. 91, 29–44.
Bowman, D., Goldsmith, V., 1983. Bar morphology of dissipative beaches: an empirical model. Mar. Geol. 51 (1–2), 15–33.
Castelle, B., Bourget, J., Molnar, N., Strauss, D., Deschamps, S., Tomlinson, R.B., 2007. Dynamics of a wave-dominated tidal inlet and its influence on adjacent beaches, Currumbin Creek, Gold Coast, Australia. Coast. Eng. 54, 77–90.
Cheng, J., Wang, P., 2015A. Extracting turbulence under breaking waves in the surf zone. J. Waterw. Port. Coast., Ocean Eng. 141 (6), 06015003–1-06015003-10.
Cheng, J., Wang, P., 2015B. Measuring and modeling beach-profile response to tropical storm Debby, west central Florida. Proceedings of Coastal Sediments. World Scientific.
Cheng, J., Wang, P., Guo, Q.D., 2016Aa. Measuring beach profiles along a low-wave energy microtidal coast, west-central Florida, USA. Geosciences 6 (4), 44.
Cheng, J., Wang, P., Smith, R.E., 2016Bb. Hydrodynamic conditions associated with an onshore migrating and stable sandbar. J. Coast. Res. 32 (1), 153–163.
Certain, R., Barusseau, J.P., 2005. Conceptual modelling of sand bars morphodynamics for a microtidal beach (Sete, France). Bull. Soc. Geol. Fr. 176 (4), 343–354.
Davis, R.A., Barnard, P., 2003. Morphodynamics of the barrier-inlet system, west-central

Florida. Mar. Geol. 200, 77–101.
De Schipper, M.A., De Vries, S., Ruessink, B.G., De Zeeuw, R.C., Rutten, J., Van Gelder-Maas, C., Stive, M.J.F., 2016. Initial spreading of a mega feeder nourishment: observations of the Sand Engine pilot project. Coast. Eng. 111, 23–38.
Dubarbier, B., Castelle, B., Marieu, V., Ruessink, G., 2015. Process-based modeling of cross-shore sandbar behavior. Coast. Eng. 95, 35–50.
Elko, N.A., Wang, P., 2007. Immediate profile and planform evolution of a beach nourishment project with hurricane influences. Coast. Eng. 54 (1), 49–66.
Feng, Z., Reniers, A.J.H.M., Haus, B.K., Solo-Gabriele, H.M., 2013. Modeling sediment-related enterococci loading, transport, and inactivation at an embayed nonpoint source beach. Water Resour. Res. 49, 693–712.
Florida Department of Environmental Protection, 2011. Critically eroded beaches in Florida, report. Bureau of Beaches and coastal systems. Div. Water Resour. Manag. 77.
Fernández-Mora, A., Calvete, D., Falqués, A., Swart, H.E., 2015. Onshore sandbar migration in the surf zone: new insights into the wave-induced sediment transport mechanisms. Geophys. Res. Lett. 42, 2869–2877. http://dx.doi.org/10.1002/2014GL063004.
Gibeaut, J.C., Davis, R.A., 1993. Statistical Geomorphic classification of ebb-tidal deltas along the west-central Florida coast. J. Coastal Res. 18, 165–184.
Guillén, J., Palanques, A., 1993. Longshore bar and through systems in a microtidal, storm-wave dominated coast: the Ebro Delta (NW Mediterranean). Mar. Geol. 115, 239–252.
Hardle, W., Simar, L., 2003. Applied Multivariate Statistical Analysis. Springer-Verlag, Berlin, Germany, pp. 486.
Hoefel, F., Elgar, S., 2003. Wave-induced sediment transport and sandbar migration. Science 299 (5614), 1885–1887.
Holman, R.A., Sallenger, A.H., 1993. Bar generation a discussion of the duck experiments series. J. Coast. Res. 15, 76–95.
King, C.A.M., Williams, W.W., 1949. The formation and movement of sand bars by wave action. Geogr. J. 113, 69–85.
Kuriyama, Y., Ito, Y., Yanagishima, S., 2008. Medium-term variations of bar properties and their linkages with environmental factors at Hasaki, Japan. Mar. Geol. 248 (1–2), 1–10.
Kroon, A., Hoekstra, P., Houwman, K.T., Ruessink, B.G., 1994. Morphologicalmonitoring of a shoreface nourishment — NOURTEC experiment at Terschelling, The Netherlands.Proceedings, Coastal Engineering 1994. American Society of Civil Engineers, pp. 2222–2236.
Larson, M., Capobianco, M., Hanson, H., 2000. Relationship between beach profiles and waves at Duck, North Carolina, determined by canonical correlation analysis. Mar. Geol. 163 (1–4), 275–288.
Larson, M., Kraus, N.C., 1994. Temporal and spatial scale of beach profile change, Duck, North Carolina. Mar. Geol. 117, 75–94.
Lee, J.M., Park, J.Y., Choi, J.Y., 2013. Evaluation of sub-aerial topographic surveying techniques using Total Station and RTK-GPS for applications in macrotidal sand beach environment. J. Coast. Res. 65, 535–540.
Leonardo, D., Ruggiero, P., 2015. Regional scale sandbar variability: observations from the U.S. Pacific Northwest. Cont. Shelf Res. 95, 74–88.
Lin, L., Demirbilek, Z., Mase, H., 2011. Recent capabilities of CMS-Wave: a coastal wave model for inlets and navigation projects. J. Coast. Res. Spec. Issue 59, 7–14.
Longo, S., Petti, M., Losada, I.J., 2002. Turbulence in the swash and surf zones: a review. Coast. Eng. 45 (3–4), 129–147.
Mase, H., 2001. Multidirectional random wave transformation model based on energy balance equation. Coast. Eng. J. 43 (4), 317–337.
Ojeda, E., Guillen, J., Ribas, F., 2011. Dynamics of single barred embayed beaches. Mar. Geol. 280, 76–90.
Pape, L., Plant, N.G., Ruessink, B.G., 2010. On cross-shore migration and equilibrium states of nearshore sandbars. J. Geophys. Res. 115, F03008.
Plant, N.G., Freilich, M.H., Holman, R.A., 2001. Role of morphologic feedback in surf zone sandbar response. J. Geophys. Res. 106 (C1), 973–989.
Ruessink, B.G., Van Enckevort, I.M.M., Kingston, K.S., Davidson, M.A., 2000. Analysis of observed two- and three-dimensional nearshore bar behavior. Mar. Geol. 169, 161–183.
Ruessink, B.G., Kuriyama, Y., 2008. Numerical predictability experiments of cross-shore sandbar migration. Geophys. Res. Lett. 35, L01603.
Ruggiero, P., Walstra, D.J.R., Gelfenbaum, G., Van Ormondt, M., 2009. Seasonal-scale nearshore morphological evolution: field observations and numerical modeling. Coast. Eng. 56, 1153–1172.
Rutten, J., Ruessink, B.G., Price, T.D., 2017. Observations on sandbar behaviour along a man-made curved coast. earth surf. process. Landforms. http://dx.doi.org/10.1002/esp.4158.
Roberts, T.M., Wang, P., 2012. Four-year performance and associated controlling factors of several beach nourishment projects along three adjacent barrier island, west-central Florida, USA. Coast. Eng. 70, 21–39.
Splinter, K.D., Holman, R.A., Plant, N.G., 2011. A behavior-oriented dynamic model for sandbar migration and 2DH evolution. J. Geophys. Res. 116, C01020.
Tolman, H.L., 2014. User manual and system documentation of WAVEWATCH III version 4.18. Thchnical Report. NOAA/NWS/NCEP/MMAB.
Voulgaris, G., Collins, M.B., 2000. Sediment resuspension on beaches: response to breaking waves. Mar. Geol. 167 (1–2), 167–187.
Van Duin, M.J.P., Wiersma, N.R., Walstra, D.J.R., Van Rijn, L.C., Stive, M.J.F., 2004. Nourishing the shoreface: observations and hindcasting of the Egmond case, The Netherlands. Coast. Eng. 51, 813–837.
Walstra, D.J.R., Reniers, A.J.H.M., Ranasinghe, R., Roelvink, J.A., Ruessink, B.G., 2012. On bar growth and decay during interannual net offshore migration. Coast. Eng. 60, 190–200.
Walton, T.L., 1976. Littoral Drift Estimates along the Coastline of Florida; Florida Sea Grant Report No. 13. University of Florida, Gainesville, FL, USA.
Wang, P., Davis, R.A., 1998. A beach profile model for a barred coast-case study from sand Kye, West-central Florida. J. Coast. Res. 981–991.
Wang, P., Davis, R.A., 1999. Depth of closure and the equilibrium beach profile - A case study from sand key, West-central Florida. Shore Beach 67, 33–42.
Wang, P., Ebersole, B.A., Smith, E.R., 2003. Beach-profile evolution under spilling and plunging breakers. J. Waterw. Port. Coast. Ocean Eng. 129 (1), 41–46.
Wang, P., Beck, T.M., 2012. Morphodynamics of an anthropogenically altered dual-inlet system: john's Pass and Blind Pass, west–central Florida, USA. Mar. Geol. 291–294 (1), 162–175.
Wang, P., Cheng, J., Horwitz, M.H., Legault, K.R., 2015. Comparing two numerical models in simulating hydrodynamics and sediment transport at a dual inlet system, west-central Florida, Proceedings of Coastal Sediments 2015, World Scientific. 14.
Wang, P., Cheng J., 2017, Performance of the Pinellas County Beach Nourishment Projects along Sand Key, Treasure Island, and Long Key, Progress Report: Post-nourishment to December 2016. Progress Report, Coastal Research Laboratory, University of South Florida, Tampa, Florida, 186 pp.